

UCM: Unifying Camera Control and Memory with Time-aware Positional Encoding Warping for World Models

Tian-Xing Xu*
xutx21@mails.tsinghua.edu.cn
Tsinghua University
China

Zi-Xuan Wang*
wangzixu21@mails.tsinghua.edu.cn
Tsinghua University
China

Guangyuan Wang*[†]
yixuan.wgy@alibaba-inc.com
Tongyi Lab, Alibaba
China

Li Hu[†]
hooks.hl@alibaba-inc.com
Tongyi Lab, Alibaba
China

Zhongyi Zhang
ericzhang@mail.ustc.edu.cn
University of Science and Technology
of China
China

Peng Zhang
futian.zp@alibaba-inc.com
Tongyi Lab, Alibaba
China

Bang Zhang[‡]
bangzhang@gmail.com
Tongyi Lab, Alibaba
China

Song-Hai Zhang[‡]
shz@tsinghua.edu.cn
Tsinghua University
China



Figure 1: Visual results of our proposed UCM. Given a reference image, a user-specified camera trajectory and a prompt, UCM enables camera-controlled, long-term consistent world generation via time-aware positional encoding warping.

Abstract

World models based on video generation demonstrate remarkable potential for simulating interactive environments but face persistent difficulties in two key areas: maintaining long-term content consistency when scenes are revisited and enabling precise camera control from user-provided inputs. Existing methods based on explicit 3D reconstruction often compromise flexibility in unbounded scenarios and fine-grained structures. Alternative methods rely directly on previously generated frames without establishing explicit spatial correspondence, thereby constraining controllability and consistency. To address these limitations, we present

UCM, a novel framework that unifies long-term memory and precise camera control via a time-aware positional encoding warping mechanism. To reduce computational overhead, we design an efficient dual-stream diffusion transformer for high-fidelity generation. Moreover, we introduce a scalable data curation strategy utilizing point-cloud-based rendering to simulate scene revisiting, facilitating training on over 500K monocular videos. Extensive experiments on real-world and synthetic benchmarks demonstrate that UCM significantly outperforms state-of-the-art methods in long-term scene consistency, while also achieving precise camera controllability in high-fidelity video generation. Project Page: <https://humanaigc.github.io/ucm-webpage/>

*Co-first authors.

[†]Project leaders.

[‡]Corresponding authors.

1 Introduction

World models [1, 2, 6, 9, 12, 19, 35, 39, 45, 64] have drawn increasing attention for their capability to simulate real environments in response to user inputs, serving as a fundamental pillar for diverse interactive applications, ranging from simulation [39, 64], autonomous driving [19, 35] and robotics [2] to game engines [9, 45]. Recent advances [15, 36, 39, 51, 55] in video-generation-based world models have substantially advanced this domain, enabling high-fidelity generation of potential future scenarios through training on large-scale real-world videos. Within this paradigm, adapting powerful video generation models for world simulation confronts two core challenges: 1) maintaining long-term content consistency and 2) achieving precise user-guided camera control. Although contemporary methods [24, 61] ensure frame-to-frame temporal coherence, they frequently fail to maintain consistency when revisiting previously observed scenes—a limitation that is often attributed to the finite context window of temporal conditioning [51, 55]. Furthermore, integrating precise camera control into video generation models remains difficult, primarily due to the inherent viewpoint diversity present in open-world videos.

To address these problems, inspired by ViewCrafter [57], some method [51] employs explicit 3D scene reconstruction to preserve long-term geometry and incorporate viewpoint information. It aggregates 3D point clouds estimated from all historical frames through truncated signed distance function (TSDF) fusion [58], subsequently rendering these points from target viewpoints to condition new frame generation. However, reliance on explicit 3D representations often compromises flexibility in large-scale, unbounded scenes and can result in a loss of details, particularly for fine-grained structures.

Another pipeline conditions future video generation directly on previously generated frames, typically by concatenating them along the temporal axis. For camera controllability and inter-frame correspondence modeling, they encode either raw camera parameters [55] or Plücker embeddings [31, 52] via a learnable camera encoder, subsequently injecting them into the feature sequence for camera-controlled generation. Despite promising results, such methods rely on implicitly learned 3D priors—derived solely from 2D posed frames—to capture cross-view correspondences. This reliance on implicit priors hinders precise camera control and weakens spatial correspondence, ultimately resulting in content inconsistencies.

In this paper, we propose a novel framework, named **UCM**, which unifies precise camera control and long-term memory capability via time-aware positional encoding warping for world models. We build our method upon a diffusion transformer (DiT) based video generation model, which represents videos as visual tokens augmented with 3D positional encodings (PEs) to encapsulate spatio-temporal information. Following previous works [31, 52, 55], all historical frames serve as memory in UCM to condition the generation of subsequent sequences. Inspired by PE-Field [5], we reassign the 3D PEs of tokens from both the reference image and historical frames via a time-aware geometry-grounded warping operation. This process provides a robust, explicit spatio-temporal correspondence between tokens for camera control and memory injection. Notably, concatenating conditional tokens extends the

input sequence length. Since the 3D self-attention within DiTs has quadratic complexity with respect to this length, it thereby incurs considerable computational costs. Therefore, we present an efficient dual-stream diffusion transformer architecture designed to model conditional generation with minimal computational overhead. Another practical challenge for training is the scarcity of large-scale video datasets featuring long-term revisits of the same dynamic scenes from different viewpoints. To overcome this limitation, we implement a scalable data curation strategy that employs point-cloud-based rendering to simulate scene revisiting, enabling us leverage over 500K videos from diverse scenarios for training. This strategy significantly enhances the generalizability of our method to open-world environments.

To comprehensively evaluate our method, we collect diverse open-source videos with large camera movement from Tanks & Temples [28], RealEstate10K [63], Context-as-Memory [55] and MiraData [25], ranging from indoor to outdoor environments and realistic to synthetic styles. Our method significantly outperforms existing methods by a large margin in terms of visual quality and long-term consistency upon scene revisiting, while achieving state-of-the-art camera controllability. Extensive ablation studies validate the effectiveness of our proposed efficient dual-stream diffusion model and data curation strategy. Our contributions are summarized as follows:

- We introduce a novel time-aware positional encoding warping mechanism into world models, which establishes robust, explicit spatio-temporal correspondence between tokens to enable precise camera control and ensure long-term scene consistency.
- We present an efficient dual-stream video diffusion model for high-fidelity generation with minimal computational overhead.
- We employ a simple yet efficient data curation strategy designed to simulate long-term scene revisiting, which enables training on large-scale monocular videos and substantially improves our model’s generalization.

2 Related Works

Video generation models. The recent scaling of video datasets has substantially advanced the capabilities of video generation models, such as Sora [64], Seedance [16] and HY Video [29]. Full-sequence diffusion models [16, 29, 46, 53] have emerged as a predominant paradigm due to their high-quality generation. However, GPU memory constrains limit the length of generated videos, and these models generally lack scene consistency across multiple, distinct video clips. Alternative architectures, such as auto-regressive models [10, 17, 24, 42, 61], generate new frames conditioned on preceding outputs, thereby achieving video generation of considerable length, but are similarly constrained by a finite temporal context window, lacking long-term memory capability.

Memory for long-term video generation. Many demos [12, 26, 42] exhibit gradual scene drift due to limited context window length. To preserve long-term geometry, recent works [51] utilize 3D reconstruction model to estimate explicit 3D representations like point clouds from previously generated frames. These 3D representations are aggregated via TSDF fusion [58] to condition subsequent clip generation. However, such explicit 3D representations often lack

flexibility in large, unbounded scenes and suffer from loss of details for fine-grained structure. Other methods [31, 52, 55] conditions generation directly on retrieved historical frames, using metrics like view frustum similarity [52, 55] or 3D surfel splatting [31]. These methods depend on implicit 3D priors learned during training to model inter-frame relationships, which impedes robust long-term scene coherence across diverse scenarios.

Camera controlled video generation. Enabling video generation conditioned on explicit camera trajectories remains a central challenge for long-term generation. One line of work employs explicit 3D representations derived from an initial frame to guide image-to-video generation, utilizing techniques such as point cloud rendering [8, 14, 32, 38, 54, 56, 57, 59], tracking [18] or optical flow [7]. Alternatively, other approaches incorporate additional trainable modules into existing video diffusion models to learn the implicit frame-wise correspondence from data, conditioning on raw pose parameters [4, 50], Plücker embeddings [3, 20, 21] or relative camera encodings [60]. We argue that establishing explicit, token-level spatial correspondence offers superior camera controllability and memory capability compared to implicit conditioning, and propose to unify camera control and memory with time-aware positional encoding warping for world models.

3 Preliminaries

DiT-based video generation models. Our method is built on a pretrained image-to-video (I2V) generation model [46]. This model consists of a causal spatio-temporal Variational Autoencoder [27] (VAE), which learns compact latent representations from high-dimensional visual data, and a latent diffusion transformer [40] (DiT) that models the data distribution by iteratively denoising. Each transformer block is instantiated as a sequence of 3D self-attention to model spatio-temporal relationships, cross-attention to integrate text information, and a feed-forward network (FFN) for feature refinement. Following Rectified Flows [13], the forward diffusion process is defined as $\mathbf{x}_t = t\mathbf{x}_1 + (1-t)\mathbf{x}_0$, where \mathbf{x}_1 is the clean latent code encoded by the causal VAE, $\mathbf{x}_0 \sim \mathcal{N}(0, I)$ denotes Gaussian noise and the timestep $t \in [0, 1]$ is sampled from a pre-defined distribution. The latent transformer u_θ learns to predict the velocity field $\mathbf{v}_t = d\mathbf{x}_t/dt = \mathbf{x}_1 - \mathbf{x}_0$, which defines an ordinary differential equation (ODE), by minimizing the training objective

$$\mathcal{L}(\theta) = \mathbb{E}_{\mathbf{x}_0, \mathbf{x}_1, t} \|u_\theta(\mathbf{x}_0, \mathbf{x}_1, t) - \mathbf{v}_t\|_2^2 \quad (1)$$

Here, θ denotes the learned model weights. During inference, the network iteratively transforms a randomly sampled Gaussian noise into a clean latent, which is then decoded by the VAE to generate the final video.

Positional encoding field (PE-Field). In DiT-based image generation models, the latent code \mathbf{x} is patchified and flattened into a sequence of tokens. 2D positional encodings (PE) (specifically RoPEs [43]) are appended to each token to indicate its 2D spatial locations, primarily enforcing spatial coherence within the self-attention mechanism [5]. Motivated by this finding, PE-Field [5] formulates novel view synthesis (NVS) as image generation conditioned on the source image and relative camera transformation. It concatenates clean tokens from the source image with noisy target tokens along the sequence dimension, and reassigns the PEs of

clean tokens according to their projected positions, derived from 3D reconstruction and the target view transformation. Given that patch tokens are spatially coarser than pixel-wise warping, PE-field proposes multi-level PEs for sub-patch detail modeling to improve alignment precision, which apply different heads of attention layers with warped PEs derived from different resolution grids. Additionally, PE-field extends PEs with per-token depth values to allow DiT to perceive relative depth relationships.

4 Method

Starting from a reference image $I^r \in \mathbb{R}^{H \times W \times 3}$, we aim to leverage powerful video generation models for world simulation guided by a user-specified camera trajectory. Our method follows a clip-by-clip generation paradigm for long-term simulation, in which each clip $V = \{I_i\}_{i=1}^T \in \mathbb{R}^{T \times H \times W \times 3}$ is conditioned on either the reference image or the last frame of the preceding clip. To ensure long-term scene coherence, we follow previous approaches [31, 52, 55] by retrieving the most relevant historical frames $\{I_{h_j}\}_{j=1}^M \in \mathbb{R}^{M \times H \times W \times 3}$ with corresponding view matrices $\{c_{h_j}\}_{j=1}^M \in \mathbb{R}^{M \times 4 \times 4}$, which serve as memory to condition subsequent clip generation. The overview of our proposed UCM is illustrated in Fig. 2, which unifies camera control and memory injection with time-aware positional encoding warping (Sec. 4.1). This operation establishes robust spatio-temporal token correspondences, where the conditional information is integrated using an efficient dual-stream video diffusion architecture with minimal computational overhead (Sec. 4.2). To address the scarcity of long-term, multiple revisiting videos, we adopt a simple yet effective dataset curation strategy, facilitating model training on large-scale monocular video datasets (Sec. 4.3).

4.1 Time-aware Positional Encoding Warping

Given retrieved memory frames $\{I_{h_j}\}_{j=1}^M$ with view matrices $\{c_{h_j}\}_{j=1}^M$ and a reference frame I^r as the conditional image, our objective is to generate a high-fidelity video $V = \{I_i\}_{i=1}^T$ that adheres to a text prompt and a specific new camera trajectory. We first apply the 3D VAE and patchify operation to the memory frames, conditional image and target video for dimension compression, obtaining latent codes $\mathbf{x}_h = \{x_{h_j}\}_{j=1}^M \in \mathbb{R}^{M \times \tilde{H} \times \tilde{W} \times D}$, $\mathbf{x}^r \in \mathbb{R}^{\tilde{H} \times \tilde{W} \times D}$ and $\mathbf{x} = \{x_i\}_{i=1}^N \in \mathbb{R}^{N \times \tilde{H} \times \tilde{W} \times D}$, respectively. Supposing s and r denote the spatial and temporal compression ratios, the shape of the latent codes satisfies $\tilde{H} = H/s$, $\tilde{W} = W/s$, and $N = (T+r-1)/r$. To achieve temporal alignment between the camera trajectory and the latent sequence, we assume the view transformation matrices change uniformly within r continuous frames, applying average pooling to the input trajectory to obtain $\mathbf{c} = \{c_i\}_{i=1}^N \in \mathbb{R}^{N \times 4 \times 4}$. These latent codes are then flattened into a sequence of tokens and processed by DiT blocks, which are adapted to learn the conditional distribution

$$\mathbf{x} \sim p(\mathbf{x} | \mathbf{x}_h, \mathbf{x}^r, \mathbf{c}, c_h, w) \quad (2)$$

where w represents the user-provided text condition. Existing I2V models [29, 46] typically treat the reference image as the first frame to guide synthesis. For notational simplicity, we consider the reference image as a special historical frame $I_{h_0} = I^r$ with an associated camera pose $c_{h_0} = c_1$, forming $\bar{\mathbf{x}}_h = \{x_{h_j}\}_{j=0}^M$ and $\bar{\mathbf{c}}_h = \{c_{h_j}\}_{j=0}^M$.

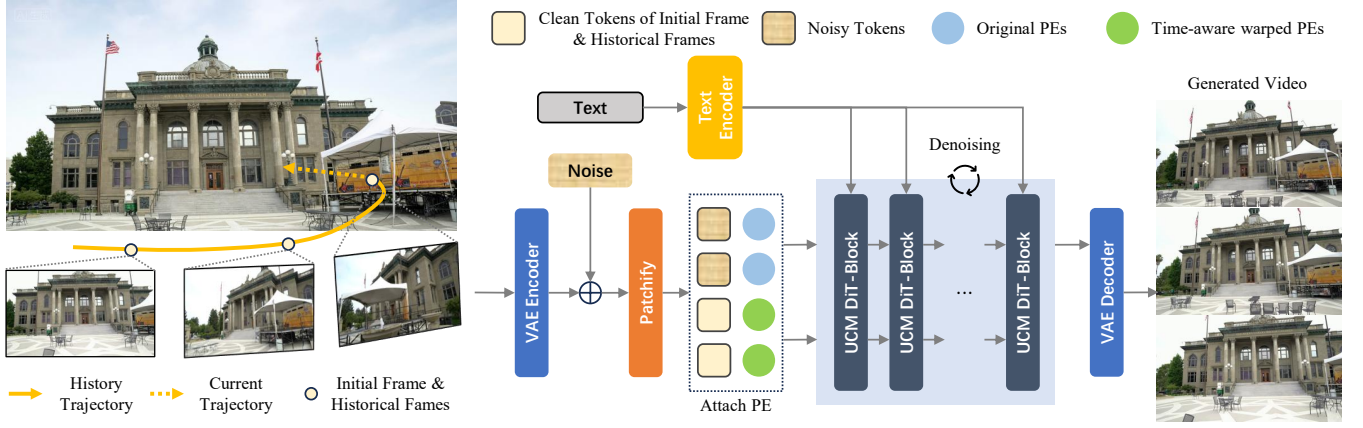


Figure 2: An overview of our proposed UCM. Given previously generated frames and a specific camera trajectory as input, UCM encodes the historical frames into clean tokens to condition the denoising of noisy tokens. For camera control and memory injection, the framework proposes time-aware positional encoding warping to establish spatio-temporal correspondence and an efficient dual-stream transformer architecture for processing. After iterative denoising, UCM yields a high-fidelity, scene-consistent video that adheres to the user-specified trajectory.

To model the relationship between the historical frames and the target views, previous works concatenate these conditional codes \bar{x}_h to the noisy codes x_t along the temporal axis before flattening, employing an auxiliary camera encoder to inject raw camera parameters [55] or Plücker embeddings [31, 52] into the generation process. These methods establish only frame-level viewpoint correspondence, relying on implicit 3D priors learned during training, thereby limiting their ability to track complex camera trajectories and maintain long-term consistency. To address this, we introduce time-aware PE warping, inspired by PE-Field [5], to unify camera control and memory for world models. Specifically, existing DiT-based methods apply 3D PEs to each visual token to capture inter-token relationships, which are obtained from their 3D coordinate (t, u, v) . We first estimate a sequence of depth maps $\{D_{h_j}\}_{j=0}^M \in \mathbb{R}^{(M+1) \times H \times W}$ for memory frames and reference image via a streaming depth estimation method [30], then lift them into point clouds $\{\mathcal{P}_{h_j}\}_{j=0}^M$ via the given view matrices \bar{c}_h through inverse perspective projection ϕ^{-1}

$$\mathcal{P}_{h_j} = \phi^{-1}(D_{h_j}, c_{h_j}) \quad (3)$$

With the point cloud \mathcal{P}_{h_j} , we can project it into the camera coordinate system of i -th target frame using the view transformation matrices c_i , obtaining warped image coordinate maps for each pixel of the historical image I_{h_j}

$$\begin{bmatrix} U_i^{h_j} \\ V_i^{h_j} \end{bmatrix} = \phi(\mathcal{P}_{h_j}, c_i) \quad (4)$$

where $U_i^{h_j}, V_i^{h_j} \in \mathbb{R}^{H \times W}$. These coordinate maps are downsampled to match the spatial resolution of the latent codes \bar{x}_h and augmented with the temporal index i to form the time-aware warped positional encoding $W_i^{h_j} = [i, U_i^{h_j}, V_i^{h_j}]$ for each conditional code x_{h_j} .

A key consideration is determining the target viewpoints for warping each conditional token x_{h_j} , because exhaustively warping to all N viewpoints would introduce unacceptable computational complexity. Thus, for frame-level camera control, we replicate the

visual code x_{h_0} of the reference image N times, warping their positional encodings to each target viewpoint c_i . For memory-guided generation, each historical frame I_{h_j} is projected only to its most relevant viewpoint k_j , obtaining the final conditional token sequence with time-aware warped PEs as

$$\left\{ \left(x_{h_0}, W_i^{h_0} \right) \right\}_{i=1}^N \cup \left\{ \left(x_{h_j}, W_{k_j}^{h_j} \right) \right\}_{j=1}^M \quad (5)$$

These conditional tokens with time-aware warped PEs are then concatenated with the noisy tokens and fed into DiT blocks to guide camera-controlled, scene-coherent video generation. Following PE-Field [5], we employ multi-level PEs to enhance sub-patch alignment precision. Unlike PE-Field, we do not explicitly incorporate depth values into the PEs, as the temporal coherence of video data enables the model to learn relative depth relationships implicitly.

4.2 Efficient Dual-stream Video Diffusion

Although the time-aware warped PEs in Eq. 5 establish strong, explicit spatio-temporal correspondence between tokens, the computational overhead from the additional tokens constrains the handling of extensive memory frames. Notably, the input tokens to the DiT can be categorized into two groups: clean tokens serve as conditioning signals to guide denoising, while noisy tokens represent the generated content and require complex modeling through iterative denoising. Building on this observation, we propose an efficient dual-stream video diffusion model, composed of sequential UCM DiT-blocks. As shown in Fig. 3, each block processes visual tokens through dual-stream 3D sparse attention, followed by a cross-attention layer to inject the text prompt and a feed-forward network (FFN) for feature refinement. For each clean token from the conditional code x_{h_j} , we restrict these tokens to attend only to other tokens from x_{h_j} , while the keys and values of these tokens are concatenated with warped time-averaged PEs to noisy tokens to guide content generation. For the noisy tokens, in addition to the inherited 3D full attention among noisy tokens, the strong

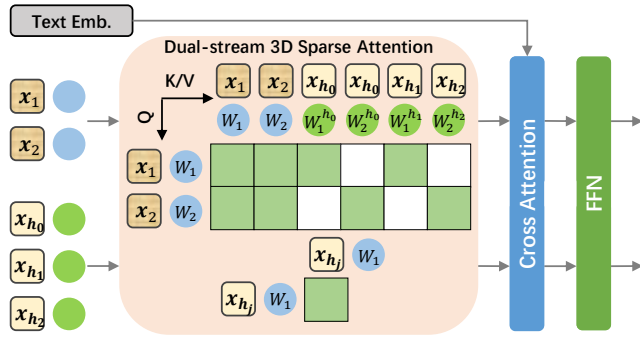


Figure 3: The architecture of UCM DiT-block. Each noisy token attends to all other noisy tokens and is guided by clean tokens via time-aware warped PEs, implemented through KV concatenation. For the clean tokens, each token attends only to other clean tokens within the same frame using original PEs. This block-sparse attention mask (here, with $k_j = j$ for visualization) enables camera control and memory guidance with reduced computational cost.

spatio-temporal correspondence provided by time-aware PE warping enables the application of a binary attention mask. This mask forces each noisy tokens, as a query, to attend only to those clean tokens warped into the same camera views. Leveraging the block sparsity of attention, our method achieves high-fidelity video generation with precise camera control and consistent content, while incurring only minimal computational overhead.

4.3 Data Curation

Training our method ideally requires long-term videos with multiple revisits to the same scene from varying viewpoints. However, existing datasets either are collected under multi-view settings [11, 34, 41], containing only static scenes without dynamic foreground objects, or are limited in scale and diversity. Alternative methods utilizing render engines like Unreal Engine 5 to synthesize multi-camera [4] or long-term revisitation videos [55] yield non-photorealistic imagery, thereby limiting model generalization to real-world data. To overcome these limitations, we adopt a simple yet effective data curation strategy, training our model on large-scale monocular videos. Given a monocular video $V = \{I_i\}_{i=1}^T$, we leverage a 3D reconstruction model [33] to obtain a sequence of point clouds $\{\mathcal{P}_i\}_{i=1}^T$ and the associated camera trajectory $\{c_i\}_{i=1}^T$. To simulate scene revisits, we randomly select several frames and render their respective point clouds \mathcal{P}_i from novel viewpoints, defined by a randomly sampled camera offset Δc . This process yields a rendered image $I'_i \in \mathbb{R}^{H \times W \times 3}$ with a binary mask $\mathcal{M}'_i \in \mathbb{R}^{H \times W}$ that indicates occluded and out-of-frame regions, as shown in Fig. 4. Since our I2V model accepts a binary mask concatenated with the latent codes as input to indicate the preserved frame, we replace it with the rendered mask \mathcal{M}'_i , explicitly informing the model which tokens from historical frames can reliably guide high-fidelity generation. For further data augmentation, we warp I'_i to frame $I_{i+\Delta i}$ with a random temporal shift Δi . This curation strategy enables the proposed UCM to achieve high-fidelity video generation with robust generalization across diverse real-world scenarios.

5 Experiments

5.1 Implementation Details

Training. Our UCM is built upon an internal I2V model finetuned from Wan2.1 1.3B-parameter T2V model [46] for comparison, supporting 81-frame (21 latent frames) video generation at a resolution of 640×352 . For training, we collect 561k monocular videos with large camera motion from Miradata [25], SpatialVID [47] and Context-as-Memory [55], ranging from real-world street views to synthetic game engine scenes, with each video comprising 801 frames. Camera poses and point clouds, required for our data curation pipeline, are annotated using the robust 3D reconstruction method Depth Anything 3 [33]. UCM is trained for 30000 iterations with an AdamW [37] optimizer at a learning rate of 3×10^{-6} . The training process is conducted on 8 NVIDIA-A100 GPUs with a mini-batch size of 8, requiring approximately four days.

Inference. During inference, we adopt SStream3R [30] to estimate a depth map for each generated frame. Following previous methods [52, 55], we retrieve 20 relevant historical frames with the co-visibility of Fields of View (FoV), defined by the Intersection of Union (IoU) ratio between target and historical camera views. For each target latent frame, we warp the most similar historical frame to its viewpoint, excluding the first latent frame, which is conditioned directly on the reference image. During sampling, we employ Classifier-Free Guidance (CFG) [23] for text prompts, with 50 sampling steps.

Evaluation. We evaluate UCM along two primary dimensions: camera controllability and long-term scene consistency. For quantitative assessment, we collect videos with large camera motion from Realestate10K [63], Tanks-and-Temples [28], and a 5% held-out subset of Context-as-Memory [55], comprising 112 diverse videos of static scenes. These videos cover diverse indoor and outdoor scenarios with both realistic and synthetic styles. For qualitative comparison, we additionally employ held-out videos of dynamic scenes from MiraData [25]. We compare our method against previous state-of-the-art methods using the following metrics:

- **Camera Control.** To quantify alignment between the camera trajectories of generated and ground-truth videos, we employ Depth Anything 3 [33] to extract camera poses from videos. Following CameraCtrl [20], camera poses are expressed relative to the first frame with normalized translation. We report the SO3 rotation distance (**RotErr**) and the L_2 translation distances (**TransErr**).
- **Visual Quality.** We calculate Fréchet Inception Distance (**FID**) [22] and Fréchet Video Distance (**FVD**) [44] between the ground truth and generated videos, for image-level and video-level quality assessment, respectively.
- **View Recall Consistency.** We employ **PSNR** [48], **SSIM** [49], and **LPIPS** [62] to measure the similarity between image pairs from identical viewpoints.

5.2 Camera Control

For camera controllability, we compare our method with previous representative video generation-based world models, including Context-as-Memory (C-a-M) [55] and VMem [31], which encode



Figure 4: Simulated revisiting from different viewpoints. We apply point cloud rendering with randomly perturbed viewpoints to simulate revisiting of the same scene for monocular videos.

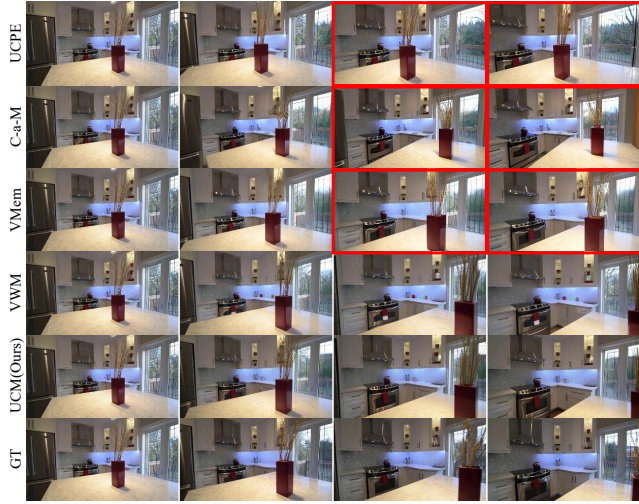


Figure 5: Visual comparison of camera controllability. We highlight imprecise camera-controlled frame generation with red boxes.

raw camera parameters and Plücker embeddings via a camera encoder to learn implicit 3D priors from data, and Video World Model (VWM) [51], which utilizes 3D point cloud renderings as conditions. Furthermore, we also evaluate the state-of-the-art relative camera encoding method UCPE [60] on 81-frame videos extracted from the videos we collected. Due to the inaccessibility of model weights [51, 55], or their unsuitability for I2V tasks [31, 60], we reimplement these methods on the same 1.3B-parameter foundational model as our approach, training with our proposed data curation strategy. As shown in Tab. 1 and Fig. 5, our method consistently outperforms previous implicit camera-controlled methods by an obvious margin, demonstrating the precise view transformation correspondence provided by time-aware positional encoding warping. While VWM also achieves state-of-the-art performance, it relies heavily on the quality of 3D representation, thereby exhibiting limitations in handling unbounded scenes and preserving fine-grained structural details, as discussed in Sec. 5.3 and shown in Fig. 7.

5.3 Long-term Memory

We compare our method with Context-as-Memory (C-a-M) [55], VMem [31] and Video World Model (VWM) [51] under two evaluation protocols, following previous method [55].

Table 1: Quantitative comparison of camera controllability. We highlight the best and second best entries.

Method	Camera Enc.	Camera Control		Visual Quality	
		RotErr (°) ↓	TransErr ↓	FID ↓	FVD ↓
UCPE	Relative Enc.	6.28	0.39	86.32	422.36
C-a-M	Raw Param.	5.45	0.46	81.99	377.56
VMem	Plücker	2.22	0.30	79.14	362.91
VWM	Point cloud	<u>1.54</u>	0.10	68.79	250.49
Ours	TPE Warping	1.01	<u>0.11</u>	<u>69.76</u>	<u>261.27</u>

- **Memory Initialization.** For each 801-frame video, we utilize the previous consecutive 480 frames as historical frames to predict the following 321 frames. We exclude videos from RealEstate10K [63] for their short durations. The quality of the 321 generated frames is assessed through direct comparison with the ground truths.
- **Cycle Trajectory.** Given the initial frame and a text prompt as conditions, we generate a long-term video that adheres to the cycle camera trajectory by making the camera return to the starting point along the same path in reverse order. For visual quality metrics, we evaluate whether newly generated frames match historical temporally symmetric generated frames.

As shown in Tab. 2, our UCM achieves the best performance under both evaluation settings, exhibiting significant improvements across all evaluation metrics. Qualitative comparisons are provided in Fig. 6 and Fig. 7. Implicit methods, such as C-a-M and VMem, lacking a token-level explicit correspondence prior, struggle to adhere faithfully to the camera trajectory and sometimes fail to preserve long-term geometry (Fig. 6, left). Although VWM also demonstrates promising camera-controllability, it relies on TSDF fusion for aggregating multi-frame point clouds, leading to inflexibility for unbounded scenes (Fig. 6, left) or fine-grained structures (Fig. 6, right; Fig. 7, right). In contrast, our method generates high-fidelity videos across both gaming and realistic scenarios with 2.4 seconds per frame on an A100 GPU, while achieving precise camera controllability and long-term scene consistency, thanks to our proposed time-aware PE warping and the efficient dual-stream video diffusion model. We also provide more visual results in Fig. 8, which demonstrates the effectiveness of our proposed method on long-term scene-consistent world generation.

5.4 Ablation Studies

Number of memory frames. We explore how the number of retrieved historical frames affects memory capability in Tab. 3. As the number of retrieved frames increases, long-term memory preservation of UCM improves under two settings with moderate computational overhead, facilitated by our proposed dual-stream video diffusion model. To balance the performance and computational cost, we retrieve 20 frames as our baseline for a good trade-off.

Efficient dual-stream video diffusion model. To demonstrate the effectiveness of dual-stream architecture and the binary block mask in 3D attention, we ablate them by 1) concatenating both the noisy tokens and conditional tokens before feeding them into the diffusion model, or 2) applying the 3D full attention for injecting conditions. As shown in Tab. 3, although ablating the dual-stream design leads to an improvement under the cycle trajectory, it also

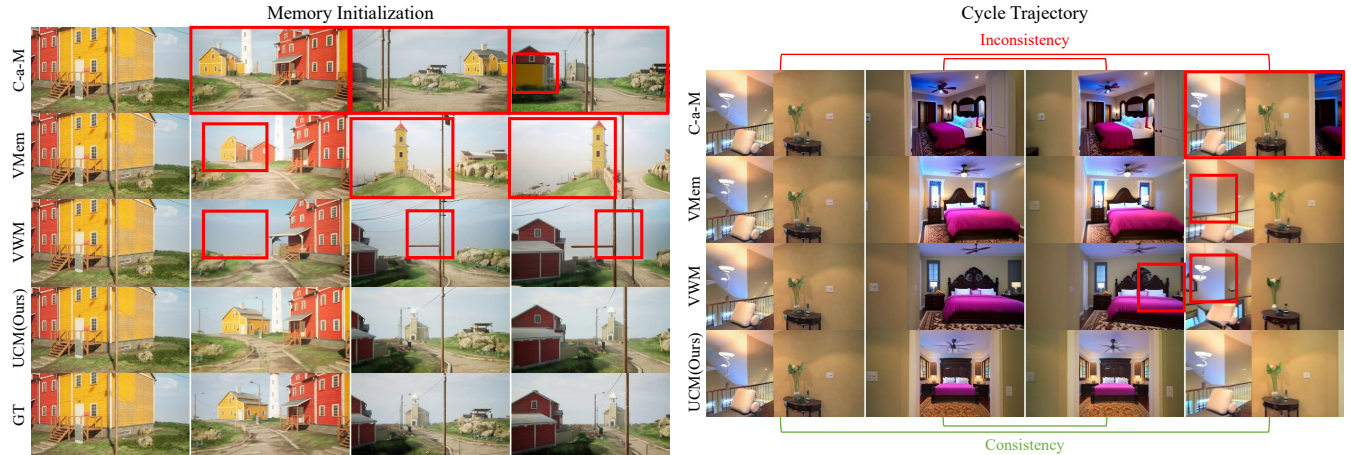


Figure 6: Visual comparison of long-term memory under two evaluation settings. Red boxes highlight obvious failure cases of camera-controlled generation or inconsistent scene generation.

Table 2: Quantitative evaluations for long-term memory persistency. We highlight the **best** and **second best** entries.

Method	Memory Initialization							Cycle Trajectory						
	Camera Control		Visual Quality		View Recall Consistency			Camera Control		Visual Quality		View Recall Consistency		
	RotErr (°) ↓	TransErr ↓	FID ↓	FVD ↓	SSIM ↑	PSNR ↑	LPIPS ↓	RotErr (°) ↓	TransErr ↓	FID ↓	FVD ↓	SSIM ↑	PSNR ↑	LPIPS ↓
C-a-M	10.87	0.39	115.17	303.34	0.35	12.44	0.56	11.50	0.52	<u>37.51</u>	138.29	0.50	15.68	0.34
VMem	5.35	0.23	<u>110.91</u>	<u>292.08</u>	0.38	12.78	0.50	4.78	0.35	<u>44.05</u>	<u>133.95</u>	0.55	16.35	0.28
VWM	<u>2.60</u>	<u>0.13</u>	115.11	301.77	<u>0.46</u>	<u>15.06</u>	<u>0.42</u>	<u>3.54</u>	<u>0.13</u>	61.43	179.72	<u>0.68</u>	<u>19.54</u>	<u>0.23</u>
Ours	2.32	0.12	83.44	198.84	0.48	15.57	0.34	3.29	0.12	21.78	61.47	0.77	23.01	0.09

Table 3: Quantitative evaluations for ablation studies on sparse attention and the number of memory frames. We highlight the **best** and **second best** entries. “Mem” indicates the number of retrieved memory frames, while “Dual” and “Sparse” represent dual-stream architecture and sparse attention, respectively. “Data” is the data curation strategy.

Mem	Dual	Sparse	Data	Memory Initialization					Cycle Trajectory					Generation Speed s/frame ↓
				Visual Quality		View Recall Consistency			Visual Quality		View Recall Consistency			
				FID ↓	FVD ↓	SSIM ↑	PSNR ↑	LPIPS ↓	FID ↓	FVD ↓	SSIM ↑	PSNR ↑	LPIPS ↓	
2	✓	✓	✓	88.24	226.35	0.47	15.43	0.36	27.81	75.25	0.65	20.14	0.15	1.72
4	✓	✓	✓	84.92	207.05	0.47	15.49	0.35	24.92	67.32	0.69	21.35	0.12	1.80
5	✓	✓	✓	85.29	213.19	0.47	15.54	0.35	24.46	68.49	0.70	21.59	0.12	1.81
10	✓	✓	✓	84.05	211.89	<u>0.48</u>	15.49	0.35	22.98	61.82	0.74	22.49	0.10	2.03
20	✓	✓	✓	<u>83.44</u>	<u>198.84</u>	<u>0.48</u>	<u>15.57</u>	0.34	23.01	58.16	<u>0.77</u>	23.57	0.09	2.40
40	✓	✓	✓	80.68	188.41	0.49	15.79	0.34	<u>18.76</u>	<u>52.72</u>	0.80	23.79	0.08	3.26
20			✓	85.05	205.43	0.47	15.32	0.35	17.13	37.55	<u>0.77</u>	<u>23.76</u>	0.08	5.14
20	✓		✓	94.72	270.09	0.47	14.30	0.37	29.28	98.49	0.73	20.42	0.12	2.94
20	✓	✓		90.65	248.87	0.48	15.08	0.35	29.53	103.46	0.74	20.74	0.11	2.40

significantly increases the computational cost and hinders practical applications. Notably, applying block attention masks not only accelerates the generation speed but also forces each token to attend its most relevant frame, resulting in an obvious performance gain.

Data curation strategy. To ablate data curation, we replace point cloud renderings with historical frames sampled from videos, leading to a consistent performance drop in terms of visual quality and recall consistency in Tab. 3. The comparison demonstrates that data curation allows our model to generate high-fidelity videos under diverse scenarios.

6 Conclusion

We present UCM, a novel approach that unifies camera control and memory mechanism with time-aware positional encoding warping for world models. To reduce the computational overhead during generation, we introduce an efficient dual-stream video diffusion model, which incorporates block attention masks for memory and camera injection. Instead of relying on scarce long-term videos with multiple revisits, we employ point cloud renderings to simulate revisiting, which enables us leverage web-scale monocular videos to train our model. Extensive evaluations demonstrate that our

method achieves high-fidelity video generation under precise camera control and long-term memory preservation, outperforming previous approaches with an obvious margin.

Limitations. Although achieving promising generation, our proposed UCM still suffers from the following limitations: 1) As shown in Fig. 8 (a)(b), over clip-by-clip sequences, minor prediction errors accumulate, potentially impeding the appearance integrity of the simulation. 2) Our method relies on learned priors to distinguish dynamic objects and static scenes during memory injection, thus sometimes suffers from artifacts caused by movable objects. 3) As the number of generated frames increases, the storage and computational overhead of streaming depth estimation methods is non-negligible. How to efficiently organize historical information will be required for practical deployment.

Acknowledgement

Tian-Xing Xu, Zi-Xuan Wang and Zhongyi Zhang completed this work during their internship at Tongyi Lab, Alibaba.

References

- [1] Eloi Alonso, Adam Jelley, Vincent Micheli, Anssi Kanervisto, Amos J Storkey, Tim Pearce, and François Fleuret. 2024. Diffusion for world modeling: Visual details matter in atari. *Advances in Neural Information Processing Systems 37* (2024), 58757–58791.
- [2] Genesis Authors. 2024. Genesis: A universal and generative physics engine for robotics and beyond, December 2024. URL <https://github.com/Genesis-Embodied-AI/Genesis> 9 (2024).
- [3] Sherwin Bahmani, Ivan Skorokhodov, Guocheng Qian, Aliaksandr Siarohin, Willi Menapace, Andrea Tagliasacchi, David B Lindell, and Sergey Tulyakov. 2025. Ac3d: Analyzing and improving 3d camera control in video diffusion transformers. In *Proceedings of the Computer Vision and Pattern Recognition Conference*. 22875–22889.
- [4] Jianhong Bai, Menghan Xia, Xiao Fu, Xintao Wang, Lianrui Mu, Jinwen Cao, ZuoZhu Liu, Haoji Hu, Xiang Bai, Pengfei Wan, et al. 2025. Recammaster: Camera-controlled generative rendering from a single video. *arXiv preprint arXiv:2503.11647* (2025).
- [5] Yunpeng Bai, Haoxiang Li, and Qixing Huang. 2025. Positional encoding field. *arXiv preprint arXiv:2510.20385* (2025).
- [6] Amir Bar, Gaoyue Zhou, Danny Tran, Trevor Darrell, and Yann LeCun. 2025. Navigation world models. In *Proceedings of the Computer Vision and Pattern Recognition Conference*. 15791–15801.
- [7] Ryan Burgert, Yuancheng Xu, Wenqi Xian, Oliver Pilarski, Pascal Clausen, Mingming He, Li Ma, Yitong Deng, Lingxiao Li, Mohsen Mousavi, et al. 2025. Go-with-the-flow: Motion-controllable video diffusion models using real-time warped noise. In *Proceedings of the Computer Vision and Pattern Recognition Conference*. 13–23.
- [8] Chenjie Cao, Jingkai Zhou, Shikai Li, Jingyun Liang, Chaohui Yu, Fan Wang, Xiangyang Xue, and Yanwei Fu. 2025. Uni3c: Unifying precisely 3d-enhanced camera and human motion controls for video generation. In *Proceedings of the SIGGRAPH Asia 2025 Conference Papers*. 1–12.
- [9] Haoxuan Che, Xuanhua He, Quande Liu, Cheng Jin, and Hao Chen. 2024. Gamegen-x: Interactive open-world game video generation. *arXiv preprint arXiv:2411.00769* (2024).
- [10] Boyuan Chen, Diego Martí Monsó, Yilun Du, Max Simchowitz, Russ Tedrake, and Vincent Sitzmann. 2024. Diffusion forcing: Next-token prediction meets full-sequence diffusion. *Advances in Neural Information Processing Systems 37* (2024), 24081–24125.
- [11] Angela Dai, Angel X Chang, Manolis Savva, Maciej Halber, Thomas Funkhouser, and Matthias Nießner. 2017. Scannet: Richly-annotated 3d reconstructions of indoor scenes. In *Proceedings of the IEEE conference on computer vision and pattern recognition*. 5828–5839.
- [12] Etched Decart, Quinn McIntyre, Spruce Campbell, Xinlei Chen, and Robert Wachen. 2024. Oasis: A universe in a transformer. URL: <https://oasis-model.github.io> (2024).
- [13] Patrick Esser, Sumith Kulal, Andreas Blattmann, Rahim Entezari, Jonas Müller, Harry Saini, Yam Levi, Dominik Lorenz, Axel Sauer, Frederic Boesel, et al. 2024. Scaling rectified flow transformers for high-resolution image synthesis. In *Forty-first international conference on machine learning*.
- [14] Wanquan Feng, Jiawei Liu, Pengqi Tu, Tianhao Qi, Mingzhen Sun, Tianxiang Ma, Songtao Zhao, Siyu Zhou, and Qian He. 2024. I2vcontrol-camera: Precise video camera control with adjustable motion strength. *arXiv preprint arXiv:2411.06525* (2024).
- [15] Jianxiong Gao, Zhaoxi Chen, Xian Liu, Junhao Zhuang, Chengming Xu, Jianfeng Feng, Yu Qiao, Yanwei Fu, Chenyang Si, and Ziwei Liu. 2025. LongVie 2: Multimodal Controllable Ultra-Long Video World Model. *arXiv preprint arXiv:2512.13604* (2025).
- [16] Yu Gao, Haoyuan Guo, Tuyen Hoang, Weilin Huang, Lu Jiang, Fangyuan Kong, Huixia Li, Jiashi Li, Liang Li, Xiaojie Li, et al. 2025. Seedance 1.0: Exploring the Boundaries of Video Generation Models. *arXiv preprint arXiv:2506.09113* (2025).
- [17] Yuchao Gu, Weijia Mao, and Mike Zheng Shou. 2025. Long-context autoregressive video modeling with next-frame prediction. *arXiv preprint arXiv:2503.19325* (2025).
- [18] Zekai Gu, Rui Yan, Jiahao Lu, Peng Li, Zhiyang Dou, Chenyang Si, Zhen Dong, Qifeng Liu, Cheng Lin, Ziwei Liu, et al. 2025. Diffusion as shader: 3d-aware video diffusion for versatile video generation control. In *Proceedings of the Special Interest Group on Computer Graphics and Interactive Techniques Conference Conference Papers*. 1–12.
- [19] Xiangyu Guo, Zhanqian Wu, Kaixin Xiong, Ziyang Xu, Lijun Zhou, Gangwei Xu, Shaoqing Xu, Haiyang Sun, Bing Wang, Guang Chen, et al. 2025. Genesis: Multimodal Driving Scene Generation with Spatio-Temporal and Cross-Modal Consistency. *arXiv preprint arXiv:2506.07497* (2025).
- [20] Hao He, Yinghao Xu, Yuwei Guo, Gordon Wetzstein, Bo Dai, Hongsheng Li, and Ceyuan Yang. 2024. Cameractrl: Enabling camera control for text-to-video generation. *arXiv preprint arXiv:2404.02101* (2024).
- [21] Hao He, Ceyuan Yang, Shanchuan Lin, Yinghao Xu, Meng Wei, Liangke Gui, Qi Zhao, Gordon Wetzstein, Lu Jiang, and Hongsheng Li. 2025. Cameractrl ii: Dynamic scene exploration via camera-controlled video diffusion models. *arXiv preprint arXiv:2503.10592* (2025).
- [22] Martin Heusel, Hubert Ramsauer, Thomas Unterthiner, Bernhard Nessler, and Sepp Hochreiter. 2017. Gans trained by a two time-scale update rule converge to a local nash equilibrium. *Advances in neural information processing systems 30* (2017).
- [23] Jonathan Ho and Tim Salimans. 2022. Classifier-Free Diffusion Guidance. *CoRR abs/2207.12598* (2022). arXiv:2207.12598 doi:10.48550/ARXIV.2207.12598
- [24] Xun Huang, Zhengqi Li, Guande He, Mingyuan Zhou, and Eli Shechtman. 2025. Self Forcing: Bridging the Train-Test Gap in Autoregressive Video Diffusion. *arXiv preprint arXiv:2506.08009* (2025).
- [25] Xuan Ju, Yiming Gao, Zhaoyang Zhang, Ziyang Yuan, Xintao Wang, Ailing Zeng, Yu Xiong, Qiang Xu, and Ying Shan. 2024. Miradata: A large-scale video dataset with long durations and structured captions. *Advances in Neural Information Processing Systems 37* (2024), 48955–48970.
- [26] Anssi Kanervisto, Dave Bignell, Linda Yilin Wen, Martin Grayson, Raluca Georgescu, Sergio Valcarcel Macua, Shan Zheng Tan, Tabish Rashid, Tim Pearce, Yuhao Cao, et al. 2025. World and human action models towards gameplay ideation. *Nature* 638, 8051 (2025), 656–663.
- [27] Diederik P Kingma and Max Welling. 2013. Auto-encoding variational bayes. *arXiv preprint arXiv:1312.6114* (2013).
- [28] Arno Knapitsch, Jaesik Park, Qian-Yi Zhou, and Vladlen Koltun. 2017. Tanks and temples: Benchmarking large-scale scene reconstruction. *ACM Transactions on Graphics (ToG)* 36, 4 (2017), 1–13.
- [29] Weijie Kong, Qi Tian, Zijian Zhang, Rox Min, ZuoZhuo Dai, Jin Zhou, Jiangfeng Xiong, Xin Li, Bo Wu, Jianwei Zhang, et al. 2024. Hunyuanvideo: A systematic framework for large video generative models. *arXiv preprint arXiv:2412.03603* (2024).
- [30] Yushi Lan, Yihang Luo, Fangzhou Hong, Shangchen Zhou, Honghua Chen, Zhaoyang Lyu, Shuai Yang, Bo Dai, Chen Change Loy, and Xingang Pan. 2025. Stream3r: Scalable sequential 3d reconstruction with causal transformer. *arXiv preprint arXiv:2508.10893* (2025).
- [31] Runjia Li, Philip Torr, Andrea Vedaldi, and Tomas Jakab. 2025. VMem: Consistent Interactive Video Scene Generation with Surfel-Indexed View Memory. *arXiv preprint arXiv:2506.18903* (2025).
- [32] Teng Li, Guangcong Zheng, Rui Jiang, Shuigen Zhan, Tao Wu, Yehao Lu, Yining Lin, Chuanyun Deng, Yepan Xiong, Min Chen, et al. 2025. Realcam-i2v: Real-world image-to-video generation with interactive complex camera control. In *Proceedings of the IEEE/CVF International Conference on Computer Vision*. 28785–28796.
- [33] Haotong Lin, Sili Chen, Junhao Liew, Donny Y Chen, Zhenyu Li, Guang Shi, Jiashi Feng, and Bingyi Kang. 2025. Depth anything 3: Recovering the visual space from any views. *arXiv preprint arXiv:2511.10647* (2025).
- [34] Lu Ling, Yichen Sheng, Zhi Tu, Wentian Zhao, Cheng Xin, Kun Wan, Lantao Yu, Qianyu Guo, Zixun Yu, Yawen Lu, et al. 2024. D13dv-10k: A large-scale scene dataset for deep learning-based 3d vision. In *Proceedings of the IEEE/CVF Conference on Computer Vision and Pattern Recognition*. 22160–22169.
- [35] Tianran Liu, Shengwen Zhao, and Nicholas Rhinehart. 2025. Towards foundational LiDAR world models with efficient latent flow matching. *arXiv preprint arXiv:2506.23434* (2025).

- [36] Yifan Liu, Zhiyuan Min, Zhenwei Wang, Junta Wu, Tengfei Wang, Yixuan Yuan, Yawei Luo, and Chunchao Guo. 2025. Worldmirror: Universal 3d world reconstruction with any-prior prompting. *arXiv preprint arXiv:2510.10726* (2025).
- [37] Ilya Loshchilov and Frank Hutter. 2017. Decoupled weight decay regularization. *arXiv preprint arXiv:1711.05101* (2017).
- [38] Baorui Ma, Huachen Gao, Haoge Deng, Zhengxiang Luo, Tiejun Huang, Lulu Tang, and Xinlong Wang. 2025. You see it, you got it: Learning 3d creation on pose-free videos at scale. In *Proceedings of the Computer Vision and Pattern Recognition Conference*. 2016–2029.
- [39] J Parker-Holder, P Ball, J Bruce, V Dasagi, K Holsheimer, C Kaplanis, A Moufarek, G Scully, J Shar, J Shi, et al. 2024. Genie 2: A large-scale foundation world model. URL: <https://deepmind.google/discover/blog/genie-2-a-large-scale-foundation-world-model> (2024).
- [40] William Peebles and Saining Xie. 2023. Scalable diffusion models with transformers. In *Proceedings of the IEEE/CVF international conference on computer vision*. 4195–4205.
- [41] Mike Roberts, Jason Ramapuram, Anurag Ranjan, Atulit Kumar, Miguel Angel Bautista, Nathan Paczan, Russ Webb, and Joshua M Susskind. 2021. Hypersim: A photorealistic synthetic dataset for holistic indoor scene understanding. In *Proceedings of the IEEE/CVF international conference on computer vision*. 10912–10922.
- [42] Kiwhan Song, Boyuan Chen, Max Simchowitz, Yilun Du, Russ Tedrake, and Vincent Sitzmann. 2025. History-guided video diffusion. *arXiv preprint arXiv:2502.06764* (2025).
- [43] Jianlin Su, Muratadha Ahmed, Yu Lu, Shengfeng Pan, Wen Bo, and Yunfeng Liu. 2024. Roformer: Enhanced transformer with rotary position embedding. *Neurocomputing* 568 (2024), 127063.
- [44] Thomas Unterthiner, Sjoerd Van Steenkiste, Karol Kurach, Raphael Marinier, Marcin Michalski, and Sylvain Gelly. 2018. Towards accurate generative models of video: A new metric & challenges. *arXiv preprint arXiv:1812.01717* (2018).
- [45] Dani Valevski, Yaniv Leviathan, Moab Arar, and Shlomi Fruchter. 2024. Diffusion models are real-time game engines. *arXiv preprint arXiv:2408.14837* (2024).
- [46] Team Wan, Ang Wang, Baole Ai, Bin Wen, Chaojie Mao, Chen-Wei Xie, Di Chen, Feiwei Yu, Haiming Zhao, Jianxiao Yang, et al. 2025. Wan: Open and advanced large-scale video generative models. *arXiv preprint arXiv:2503.20314* (2025).
- [47] Jiahao Wang, Yufeng Yuan, Rujie Zheng, Youtian Lin, Jian Gao, Lin-Zhuo Chen, Yajie Bao, Yi Zhang, Chang Zeng, Yanxi Zhou, et al. 2025. Spatialvid: A large-scale video dataset with spatial annotations. *arXiv preprint arXiv:2509.09676* (2025).
- [48] Zhou Wang and Alan C Bovik. 2002. A universal image quality index. *IEEE signal processing letters* 9, 3 (2002), 81–84.
- [49] Zhou Wang, Alan C Bovik, Hamid R Sheikh, and Eero P Simoncelli. 2004. Image quality assessment: from error visibility to structural similarity. *IEEE transactions on image processing* 13, 4 (2004), 600–612.
- [50] Zhouxia Wang, Ziyang Yuan, Xintao Wang, Yaowei Li, Tianshui Chen, Menghan Xia, Ping Luo, and Ying Shan. 2024. Motionctrl: A unified and flexible motion controller for video generation. In *ACM SIGGRAPH 2024 Conference Papers*. 1–11.
- [51] Tong Wu, Shuai Yang, Ryan Po, Yinghao Xu, Ziwei Liu, Dahua Lin, and Gordon Wetzstein. 2025. Video World Models with Long-term Spatial Memory. *arXiv preprint arXiv:2506.05284* (2025).
- [52] Zeqi Xiao, Yushi Lan, Yifan Zhou, Wenqi Ouyang, Shuai Yang, Yanhong Zeng, and Xingang Pan. 2025. Worldmem: Long-term consistent world simulation with memory. *arXiv preprint arXiv:2504.12369* (2025).
- [53] Zhuoyi Yang, Jiayan Teng, Wendi Zheng, Ming Ding, Shiyu Huang, Jiazheng Xu, Yuanming Yang, Wenyi Hong, Xiaohan Zhang, Guanyu Feng, et al. 2024. Cogvideox: Text-to-video diffusion models with an expert transformer. *arXiv preprint arXiv:2408.06072* (2024).
- [54] Meng You, Zhiyu Zhu, Hui Liu, and Junhui Hou. 2024. Nvs-solver: Video diffusion model as zero-shot novel view synthesizer. *arXiv preprint arXiv:2405.15364* (2024).
- [55] Jiwen Yu, Jianhong Bai, Yiran Qin, Quande Liu, Xintao Wang, Pengfei Wan, Di Zhang, and Xihui Liu. 2025. Context as memory: Scene-consistent interactive long video generation with memory retrieval. *arXiv preprint arXiv:2506.03141* (2025).
- [56] Mark YU, Wenbo Hu, Jinbo Xing, and Ying Shan. 2025. Trajectorycrafter: Redirection camera trajectory for monocular videos via diffusion models. *arXiv preprint arXiv:2503.05638* (2025).
- [57] Wangbo Yu, Jinbo Xing, Li Yuan, Wenbo Hu, Xiaoyu Li, Zhipeng Huang, Xiangjun Gao, Tien-Tsin Wong, Ying Shan, and Yonghong Tian. 2024. Viewcrafter: Taming video diffusion models for high-fidelity novel view synthesis. *arXiv preprint arXiv:2409.02048* (2024).
- [58] Andy Zeng, Shuran Song, Matthias Nießner, Matthew Fisher, Jianxiong Xiao, and Thomas A. Funkhouser. 2017. 3DMatch: Learning Local Geometric Descriptors from RGB-D Reconstructions. In *2017 IEEE Conference on Computer Vision and Pattern Recognition, CVPR 2017, Honolulu, HI, USA, July 21–26, 2017*. IEEE Computer Society, 199–208. doi:10.1109/CVPR.2017.29
- [59] Shangjin Zhai, Zhichao Ye, Jialin Liu, Weijian Xie, Jiaqi Hu, Zhen Peng, Hua Xue, Danpeng Chen, Xiaomeng Wang, Lei Yang, et al. 2025. Stargen: A spatiotemporal autoregression framework with video diffusion model for scalable and controllable scene generation. In *Proceedings of the Computer Vision and Pattern Recognition Conference*. 26822–26833.
- [60] Cheng Zhang, Boying Li, Meng Wei, Yan-Pei Cao, Camilo Cruz Gambardella, Dinh Phung, and Jianfei Cai. 2025. Unified Camera Positional Encoding for Controlled Video Generation. *arXiv preprint arXiv:2512.07237* (2025).
- [61] Lvmin Zhang and Maneesh Agrawala. 2025. Packing input frame context in next-frame prediction models for video generation. *arXiv preprint arXiv:2504.12626* (2025).
- [62] Richard Zhang, Phillip Isola, Alexei A Efros, Eli Shechtman, and Oliver Wang. 2018. The unreasonable effectiveness of deep features as a perceptual metric. In *Proceedings of the IEEE conference on computer vision and pattern recognition*. 586–595.
- [63] Tinghui Zhou, Richard Tucker, John Flynn, Graham Fyffe, and Noah Snavely. 2018. Stereo magnification: Learning view synthesis using multiplane images. *arXiv preprint arXiv:1805.09817* (2018).
- [64] Zheng Zhu, Xiaofeng Wang, Wangbo Zhao, Chen Min, Bohan Li, Nianchen Deng, Min Dou, Yuqi Wang, Botian Shi, Kai Wang, et al. 2024. Is sora a world simulator? a comprehensive survey on general world models and beyond. *arXiv preprint arXiv:2405.03520* (2024).

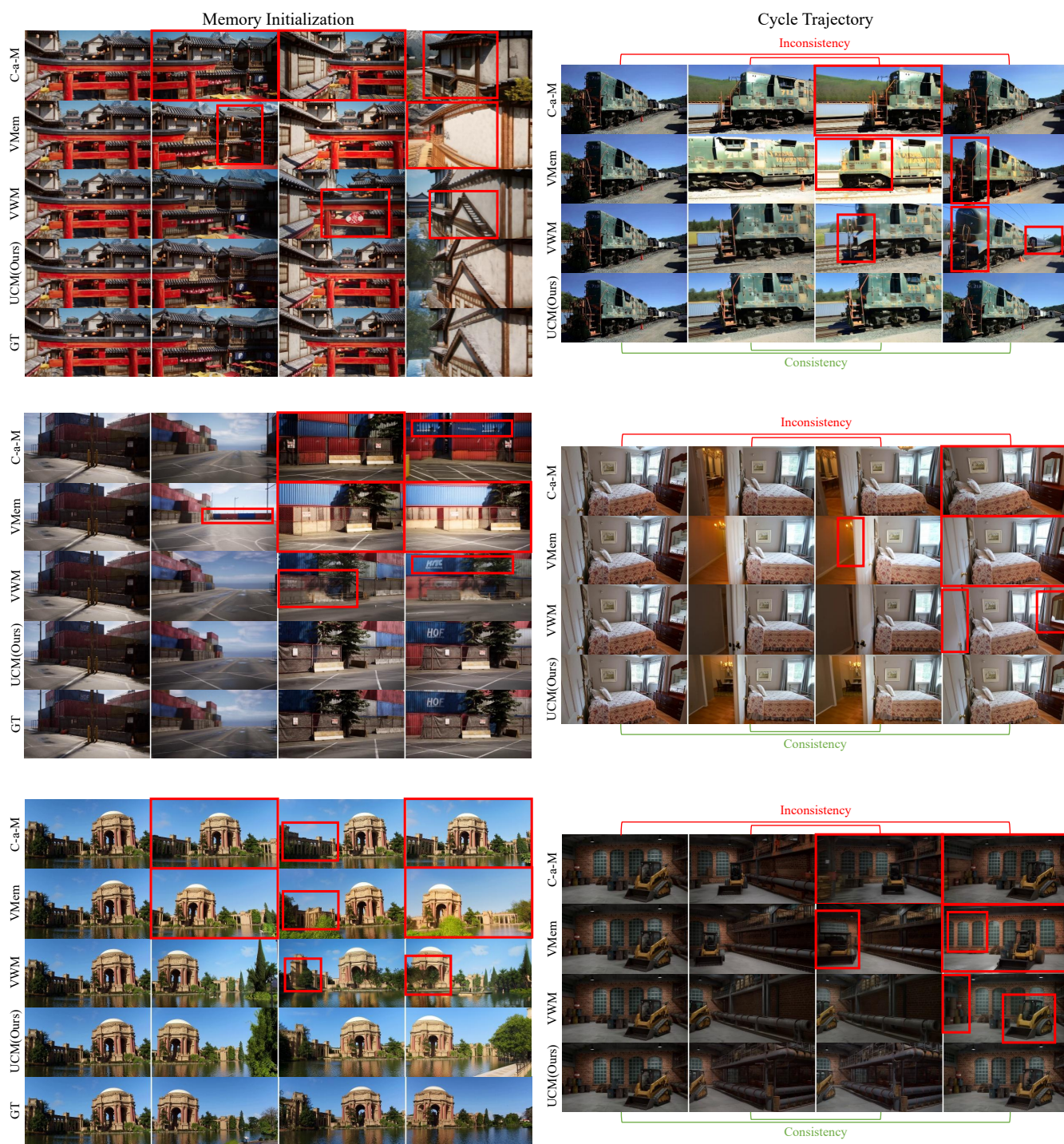


Figure 7: Supplementary visual comparison of long-term memory preservation. Red boxes indicate inaccurate camera control or scene inconsistency during generation.



(a) **Prompt:** *A rider in dark clothing follows a trail on horseback through the wilderness. Under cloudy skies, misty mountains stand quietly over the rocky land...*



(b) **Prompt:** *A lone rider in dark medieval armor, with two swords on his back, gallops across a vibrant meadow blooming with yellow, pink, and purple wildflowers...*



(c) **Prompt:** *A long-haired man with a crossbow walks carefully through a rocky, snowy path, under misty mountains and swaying bamboo, in a still and watchful moment...*



(d) **Prompt:** *A serene traditional Dutch village basks in the sunshine, with rows of red-roofed brick houses lining a cobblestone street and a small canal, all under a clear blue sky...*



(e) **Prompt:** *A quiet Japanese residential street glows in the soft evening light, lined with houses and apartment buildings in warm tones. A few parked cars sit along the curbs under a pastel sky...*



(f) **Prompt:** *A beige building with blue-trimmed windows and a balcony stands along a quiet street. Overhead power lines crisscross against a backdrop of distant snow-capped mountains...*



(g) **Prompt:** *A modern kitchen with warm wood cabinets and dark gray counters features a central island and a dining area under an elephant painting...*



(h) **Prompt:** *Sunlight fills an open living space with a brown leather sectional and patterned rug. A visible kitchen island and a white staircase complete the bright, contemporary design...*



(i) **Prompt:** *An elegant dining room centers around a dark wood table with eight beige chairs under a geometric chandelier. Glass doors open to a patio on the left...*

Figure 8: Supplementary visual results of our proposed UCM. Starting from a reference image, UCM can generate long-term videos that maintain scene consistency when viewing the same scene from different viewpoints.